Demonstration of Alternative Fabrication Techniques for Robust MEMS Device

Sung Pil Chang[a], Je Young Park, and Doo Yeol Cha
Department of Electonic Engineering, Inha University,
253 Younghyun3-dong, Nam-gu, Incheon 402-751, Korea

Heung Shik Lee
Department of Mechanical Engineering, Inha University,
253 Younghyun3-dong, Nam-gu, Incheon 402-751, Korea

[a]E-mail : spchang@inha.ac.kr

(Received July 11 2006, Accepted August 16 2006)

This work describes efforts in the fabrication and testing of robust microelectromechanical systems (MEMS). Robustness is typically achieved by investigating non-silicon substrates and materials for MEMS fabrication. Some of the traditional MEMS fabrication techniques are applicable to robust MEMS, while other techniques are drawn from other technology areas, such as electronic packaging. The fabrication technologies appropriate for robust MEMS are illustrated through laminated polymer membrane based pressure sensor arrays. Each array uses a stainless steel substrate, a laminated polymer film as a suspended movable plate, and a fixed, surface micromachined back electrode of electroplated nickel. Over an applied pressure range from 0 to 34 kPa, the net capacitance change was approximately 0.14 pF. An important attribute of this design is that only the steel substrate and the pressure sensor inlet is exposed to the flow; i.e., the sensor is self-packaged.

Keywords : MEMS, Robustness, Micro fabrication, Capacitive pressure sensor, Lamination

1. INTRODUCTION

Microelectromechanical systems (MEMS) have been primarily realized using silicon substrate because the root of micro-machining technology is in integrated circuit processing technology[1-4]. However, the use of traditional silicon-substrate micromachined devices may be limited in many applications, for example by the lack of ability of the surrounding silicon substrate to absorb large mechanical shocks. Therefore, if silicon based devices are to be used in applications where they are exposed to mechanically harsh environments, they need a robust packaging material to protect the devices from the environments[5,6].

In this work, we have investigated the use of more robust substrates as suitable starting points for both bulk and surface micromachined structures, as well as investigated the possibility of the substrate forming essential structural components of the device package. In order to alleviate parasitic effects encountered in the capacitive pressure sensor approach, the capacitive pressure sensors and the read-out chip are directly integrated on the same substrate by connecting the chip to the sensors using lithographically defined traces as in Fig. 1. This integration allows for buffering and reduction of the parasitic effects as well as the possibility of multiplexing or conversion of capacitances to frequency or voltage.

Alternative fabrication techniques, such as techniques more commonly used in either conventional machining as well as electronic packaging fabrication (e.g., lamination), are combined with more traditional integrated-circuit-based microelectronics processing techniques to create micromachined devices on or from these robust substrates.

One of the advantages of the use of robust substrates is the possibility of co-fabrication of the micromachined devices and their packages using, e.g., the robust substrate itself as an integral part of the sensor package. Another advantage is that due to substrate robustness, these co-packaged devices may be able to be used in mechanically harsh environments, such as aerospace and oceanography applications.

To illustrate these principles, a robust capacitive pressure sensor array has been fabricated using stainless steel as a substrate, Kapton polyimide film as a pressure-sensitive flexible plate, and electroplated nickel as a back electrode. An important attribute of this design is that only the stainless steel substrate and the pressure sensor inlet are exposed to the flow; i.e., the sensor is self-packaged.

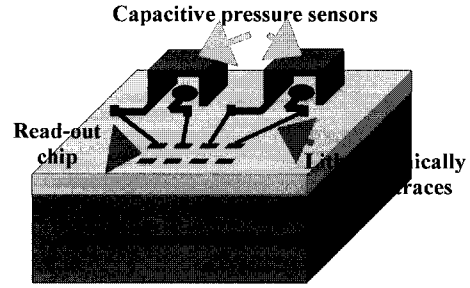

Fig. 1. An example of integrated robust capacitive pressure sensors.

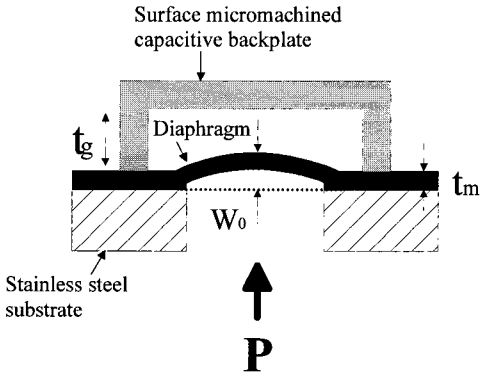

Fig. 2. A schematic diagram of the side-view of the capacitive pressure sensor.

2. THOERY AND DESIGN

The principle of operation is based on the pressure-induced deflection of a diaphragm and the subsequent measurement of the capacitance between this deflecting diaphragm and a fixed backplate surface micromachined over the deflecting diaphragm.

Figure 2 shows a schematic cross-section of the device, where t_g is the initial (undeflected) gap distance between the fixed back electrode and the diaphragm electrode, w_o is the deflection at the center of the diaphragm, t_m is the thickness of the diaphragm, and P is the uniform applied pressure.

The sensor is modeled with an electromechanical model. For mechanical modeling, several assumptions have been made: (a) the diaphragm has isotropic micromachined properties; (b) stretching of the diaphragm has been neglected, since the diaphragm does not undergo large deflections compared to its thickness; (c) the thickness of the metallic electrode on the plate has been neglected, since this thickness is small compared with the plate thickness; (d) electric field fringing effects have been neglected, since the gap between the flexible diaphragm and the fixed backplate is small compared to their lateral extents; and (e) residual stress in the diaphragm can be neglected.

Under these conditions, the deflection of a circular diaphragm with fully clamped perimeter as a function of radius, w(r), is given by[7,8]:

$$w(r) = w_0\left[1-\left(\frac{r}{a}\right)^2\right]^2 \tag{1}$$

where a is the radius of the plate. The center deflection of the plate w_0 is given by

$$w_0 = \frac{3Pa^4\left(1-\mu^2\right)}{16Et_m^3} \tag{2}$$

where E is the modulus of elasticity and μ is the Poisson ratio of the plate.

As the electric field fringing effect is neglected under the assumption (d), the electric field lines are perpendicular to the surface of the back plate and the capacitance can be expressed as a function of the shape function w(r) of the membrane by

$$C_s = \varepsilon_0 \int_0^{2\pi} d\theta \int_0^{r} dr \frac{r}{t_g - w(r)} \tag{3}$$

We replace w(r) in Equation 3 using Equation 1 and replace w_0 by the dimensionless parameter

$$\gamma = \frac{w_0}{t_g} \tag{4}$$

Then we replace the integration variable r by the dimensionless variable

$$x = \sqrt{\gamma}\left[1-\left(\frac{r}{a}\right)^2\right] \tag{5}$$

This yields

$$C = \varepsilon_0 \frac{\pi a^2}{t_g}\gamma^{-0.5}\int_0^{\sqrt{\gamma}} \frac{dx}{1-x^2} \tag{6}$$

Finally, we solve the integral and use the capacitance when the membrane is undeflected

$$C_0 = \varepsilon_0 \frac{\pi a^2}{t_g} \tag{7}$$

which yields:

$$C = C_0\gamma^{-0.5}\tanh^{-1}\left(\gamma^{0.5}\right) \approx C_0\left(1+\frac{\gamma}{3}+\frac{\gamma^2}{5}\right) \quad (8)$$

where the second part of Equation 8 was obtained from the fifth order Taylor series expansion of $\tanh^{-1}(y)$.

3. FABRICATION AND MEASUREMENT

The fabrication sequence of the capacitive pressure sensor array is shown in Fig. 3.

The process starts on square 5.7 cm (2 ¼ inch) on a side, 0.5 mm thick stainless steel substrate that has surface roughness of approximately 6-8 μm. An array of 8x8 pressure inlet holes with a diameter of 2 mm, with 5 mm center-to-center distances, is milled through the stainless steel substrate (Fig. 3(a)).

Kapton polyimide film (Dupont, Kapton HN200, 50 μm thick) is laminated onto the milled stainless steel substrate using a hot press with a pressure of 8.65 MPa and a temperature of 175 °C for 30 min (Fig. 3(b)). The laminate adhesive is an epoxy-based resin designed for printed wiring board fabrication (EIS epoxy laminate prepreg #106).

Fig. 4 shows the schematic diagram of lamination process with stainless steel substrate and Kapton polyimide film using a hot press. The pressure-sensitive diaphragms will be the kapton polyimide film in the regions suspended over the milled pressure inlet holes.

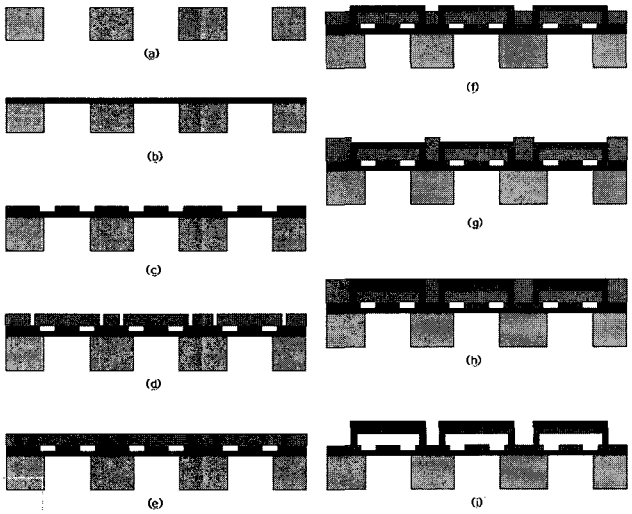

Fig. 3. Fabrication sequence of pressure sensor based on kapton polyimide diaphragm.

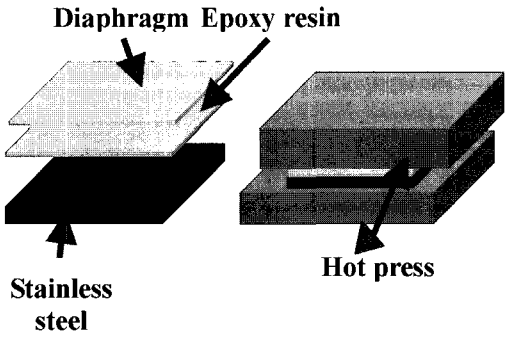

Fig. 4. A schematic diagram of lamination process with stainless steel substrate and Kapton polyimide film.

A triple metallic layer of Ti/Cu/Ti with a thickness of 100/2000/500 Å is deposited by electron-beam evaporation and then patterned using a standard lift-off process to create bottom electrodes, electroplating seed layers, and bonding pads on the surface of the kapton polyimide film (Fig. 3(c)).

Multiple layers of PI2611 polyimide (Dupont) are spun onto the patterned layer with a spin speed of 1,200 rpm for 60 seconds, and hard-cured in a N_2 ambient at 200 °C for 120 min yielding a final thickness of polyimide of approximately 44~48 μm. The polyimide layer is anisotropically etched using reactive ion etching to create electroplating molds for the support posts of the fixed backplates, and to remove the uppermost titanium layer of the seed layer (Fig. 3(d)).

Nickel supports are then electroplated through the polyimide molds (Fig. 3(e)). A Ti/Cu/Ti metallic triple layer with a thickness of 300/2000/300 Å is deposited using DC sputtering to act as a seed layer for the deposition of the backplate (Fig. 3(f)). Thick photoresist (Shipley SJR 5740) is spun on the seed layer with a spin speed of 1100 rpm for 30 seconds (yielding a final thickness of approximately 15 μm) and patterned to act as electroplating molds for the backplates (Fig. 3(g)).

After removal of the uppermost Ti layer, nickel is electroplated through the thick photoresist electroplating molds to create the backplates (Fig. 3(h)). The thick photoresist electroplating molds and the remaining seed layer is removed.

Finally, the polyimide molds for the backplate posts as well as polyimide sacrificial layers are isotropically etched to create air gaps between the fixed backplates and the pressure sensitive kapton polyimide flexible diaphragms (Fig. 3(i)). The isotropic dry etch is carried out in a barrel plasma etcher using CF_4/O_2 plasma with a RF power of 120 W. Figure 5 shows photographs of a fabricated pressure sensor array.

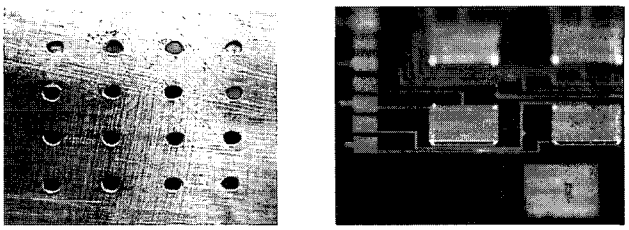

(a) (b)

Fig. 5. Photomicrographs of fabricated pressure sensors. (a) side exposed to flow, (b) sensor view.

4. CHARACTERIZATION RESULTS

The capacitance of individual pressure sensors has been measured using a Keithley 3322 LCZ meter. Measured capacitances for undeflected pressure sensors were in the range from 11.35 pF to 13.97 pF depending on the length of interconnections between bonding pads and sensors.

It has been observed that capacitance monotonically increases with increasing applied pressure, meaning that the pressure sensitive Kapton plate deflects toward the fixed backplates.

Over an applied pressure range from 0 to 34 kPa, the net capacitance change was approximately 0.14 pF. Theoretical prediction of the sensor behavior is determined by taking the first three terms of equation (8). Theoretical and measured net capacitance change over the applied pressure range are compared in Fig. 6.

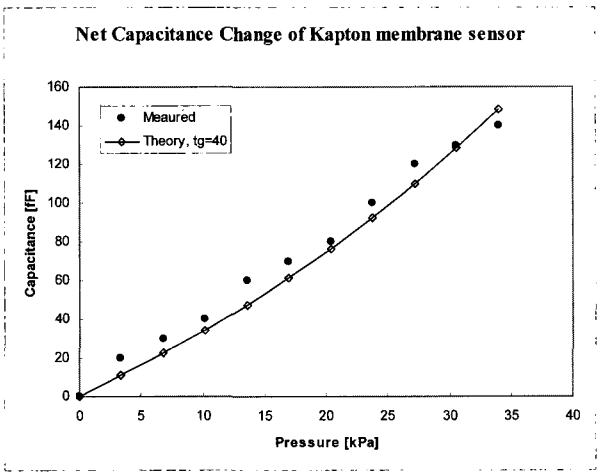

Fig. 6. A comparison of theoretical and measured values of net capacitance change over the full range of applied pressure ranging from 0 to 34 kPa.

And an OP-amp-based astable multivibrator circuit has been integrated with the pressure sensors in a hybrid fashion to create a frequency-modulated voltage output. Figure 7 shows a schematic diagram of such an astable multivibrator circuit, which consists of an LF351 operational amplifier, and three external resistors. The capacitance of the pressure sensor is the frequency-determining capacitance, which modulates the frequency of the voltage output on the output of the amplifier. The output frequency of the OP-amp is given by[9]:

$$f = \frac{1}{2RC_{sensor} \ln 3} \tag{9}$$

where RC_{sensor} is the time constant of the circuitry.

In this work, external resistors R and R_1 have been selected as 1 MΩ, resulting in a base frequency of 12.544 kHz for the output of the OP-amp. Figure 8 shows the frequency output of the OP-amp circuit as a function of applied pressure from 0 to 30 kPa. The measured value of relative frequency change is 0.93 % over the applied pressure range from 0 to 30 kPa.

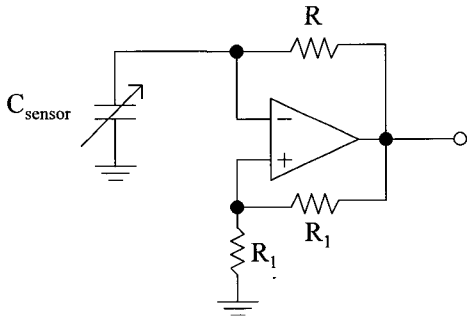

Fig. 7. Schematic diagram of the astable multivibrator circuit.

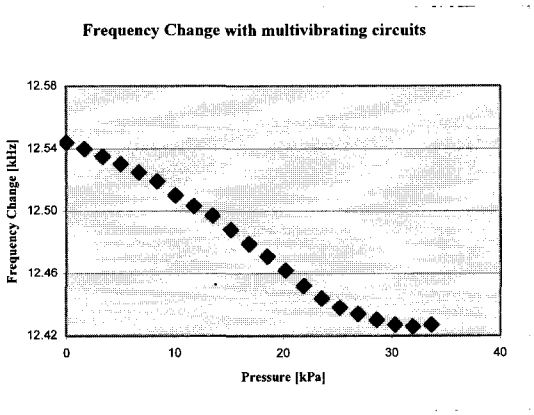

Fig. 8. The frequency output of the Op-amp circuit as a function of applied pressure from 0 to 34 KPa for the kapton pressure sensor.

5. CONCULTION

Robust materials have been studied as suitable substrates for micromachined devices. Lamination using a hot press, combined with traditional micromachining processes, has been investigated as a suitable fabrication process for the robust substrates.

A capacitive pressure sensor array using a robust substrate (0.5 mm thick stainless steel shim stock), Kapton HN200 flexible plate, and lamination processing has been designed, fabricated, and characterized. Over the applied pressure range from 0 to 34 kPa, the net capacitance change of the pressure sensor is approximately 0.14 pF. OP-amp-based multivibrator circuitry has been integrated with pressure sensors in a hybrid manner to create frequency-modulated outputs.

ACKNOWLEDGMENTS

This work was supported by INHA UNIVERSITY Research Grant(INHA-2006).

REFERENCES

[1] T. Müller, M. Brandl, O. Brand, and H. Baltes, "An industrial CMOS process family adapted for the fabrication of smart silicon sensors", Sensors and Actuators A, Vol. 84, p. 126, 2000.

[2] Von Arx, M., Paul, O., and Baltes, H., "Process-dependent thin-film thermal conductivities for thermal CMOS MEMS", Journal of Micro-electromechanical Systems, Vol. 9, No. 1, p. 136, 2000.

[3] K. Kasten, N. Kordas, H. Kappert, and W. Mokwa, "Capacitive pressure sensor with monolithically integrated CMOS readout circuit for high temperature applications", Sensors and Actuators A, Vol. 97-98, p. 83, 2003.

[4] J. S. Chae, Kulah, H., and Najafi, K., "A monolithic three-axis micro-g micromachined silicon capacitive accelerometer", Journal of Microelectromechanical Systems, Vol. 14, No. 2, p. 235, 2005.

[5] G. Kaltsas and A. G. Nassiopoulou, "Gas flow meter for application in medical equipment for respiratory control: study of the housing", Sensors and Actuators A, Vol. 110, p. 413, 2004.

[6] M. X. Chen, X. J. Yi, Z. Y. Gan, and S. Liu, "Reliability of anodically bonded silicon-glass packages", Sensors and Actuators A, Vol. 120, p. 291, 2005.

[7] W. H. Ko, M. H. Bao, and Y. D. Hong, "A high-sensitivity integrated-circuit capacitive pressure transducer", IEEE Trans. Electron Devices, Vol. ED-29, No. 1, p. 48, 1982.

[8] S. Timoshenko, "Theory of Plates and Shells", McGraw-Hill Book Company, New York, 1940.

[9] A. S. Sedra and K. C. Smith, "Microelectronic Circuits", CBS College Publishing, New York, 1982.